

## Supporting Information

# Mo<sup>IV</sup>-Polyoxomolybdates with Frustrated Lewis Pairs For High-Performance Hydrogenation Catalysis

Benlong Luo,<sup>a,b</sup> Ruili Sang,<sup>a</sup> Lifang Lin,<sup>ab</sup> Li Xu<sup>a\*</sup>

<sup>a</sup>State Key Laboratory of Structural Chemistry, Fujian Institute of Research on the Structure of Matter, Chinese Academy of Sciences, Fuzhou, Fujian, 350002.

<sup>b</sup>University of Chinese Academy of Sciences, Beijing, 100049, China.

xli@fjirsm.ac.cn

## 1. Experimental Section

### 1.1 Methods and Materials

All chemicals were obtained from commercial sources and used without further purification. Elemental analyses (C, H and N) were performed using a vario MICRO elemental analyzer. IR spectra were recorded with a Magna 750 FTIR spectrometer photometer as KBr pellets in the 4000–400 cm<sup>-1</sup> region. Conversion and yield was measured with a Shimadzu GC 2012 plus chromatograph. The X-ray photoelectron spectroscopy (XPS) measurements were carried out on a ESCALAB 250Xi spectrometer equipped with an Al K<sub>α</sub> X-ray source. The binding energy (BE) was calibrated with the C1s signal (284.6 eV) as are referenced. The thermogravimetric analyses (TGA) were performed on a Netzsch STA449C apparatus in N<sub>2</sub> atmosphere in 30–800°C. The intensity data were collected on a Bruker D8-venture diffractometer with graphite-monochromated MoK<sub>α</sub> radiation (λ = 0.71073 Å) for **1**. All absorption corrections were performed using multiscan. The structures were solved by direct methods and refined by full-matrix least-squares on F<sup>2</sup> with the SHELXTL-2016<sup>27</sup> program package. All <sup>1</sup>H and <sup>13</sup>C NMR spectra were recorded on a Bruker-BioSpin AVANCE III instrument, at a constant temperature of 300 K.

### 1.2 Synthesis

[Mo<sup>IV</sup><sub>3</sub>O<sub>2</sub>(O<sub>2</sub>CCH<sub>3</sub>)<sub>6</sub>(H<sub>2</sub>O)<sub>3</sub>]ZnCl<sub>4</sub> (**3a**)<sup>28</sup> and (Pro<sub>4</sub>N)<sub>2</sub>[Mo<sup>IV</sup><sub>3</sub>O<sub>4</sub>(C<sub>2</sub>O<sub>4</sub>)<sub>3</sub>(H<sub>2</sub>O)<sub>3</sub>] (**4a**)<sup>29</sup> were prepared according to the published procedure. [Mo<sup>IV</sup><sub>3</sub>O<sub>2</sub>(O<sub>2</sub>CCH<sub>3</sub>)<sub>6</sub>py<sub>3</sub>]ZnCl<sub>4</sub> (**3b**) and [Pro<sub>4</sub>N]<sub>2</sub>[Mo<sup>IV</sup><sub>3</sub>O<sub>4</sub>(C<sub>2</sub>O<sub>4</sub>)<sub>3</sub>py<sub>3</sub>] (**4b**, pro = CH<sub>3</sub>CH<sub>2</sub>CH<sub>2</sub>) were prepared by ligand substitution reaction. In a typical experimental procedure, [Mo<sup>IV</sup><sub>3</sub>O<sub>2</sub>(O<sub>2</sub>CCH<sub>3</sub>)<sub>6</sub>(H<sub>2</sub>O)<sub>3</sub>]ZnCl<sub>4</sub> (**3a**) and [Pro<sub>4</sub>N]<sub>2</sub>[Mo<sup>IV</sup><sub>3</sub>O<sub>4</sub>(C<sub>2</sub>O<sub>4</sub>)<sub>3</sub>(H<sub>2</sub>O)<sub>3</sub>] (**4a**) were dissolved in pyridine solution and heated for two hours respectively. The resulting red solution was dropped to diethyl ether to produce red precipitate. The resultant mixture was filtered through celite and dried to produce the red solid of **3b** and **4b** characterized by IR (Figure S9).

Preparation of **γ-1**. [Mo<sub>3</sub>O<sub>2</sub>(O<sub>2</sub>CCH<sub>3</sub>)<sub>6</sub>(H<sub>2</sub>O)<sub>3</sub>]ZnCl<sub>4</sub>•8H<sub>2</sub>O (0.11 g, 0.1 mmol) were added to a mixture of pyridine (1 mL), DMF (9 mL), and H<sub>2</sub>O (1 mL). The resulting mixture was sealed in a 20 mL Pressure bottle and heated at 75°C for two days. The reactor was cooled to room temperature at a rate of 2K/h to produce brown cubic crystals of **γ-1** (>60% yield based on Mo). Anal. calcd. For C<sub>36</sub>H<sub>61</sub>N<sub>9</sub>Mo<sub>13</sub>O<sub>38</sub> (Mr. = 2475.15): C, 17.45; H, 2.48; N, 5.09%; Found: C, 17.55; H, 2.55; N, 4.93%. IR (KBr): 3420 s (H<sub>2</sub>O), 3073 s (py), 1607 s (py), 1448 s (py), 932 s (Mo<sup>VI</sup>=O), 841 vs. (Mo<sup>VI</sup>-Ob-Mo), 752 s ([Mo<sup>IV</sup><sub>3</sub>O<sub>4</sub>]), 644 s h (py). *Cmcm*, a = 22.9530(14), b = 24.5269(15), c = 13.6041(13) Å, V = 7658.6(10) Å<sup>3</sup>, Z = 4, R1/wR2 = 2.41/6.36% for the observed data (I ≥ 2σ(I)), R1/wR2 = 2.52/6.42%

for all data; CCDC-1575811. The disordered  $\text{HN}(\text{CH}_3)_2$  and  $\text{H}_2\text{O}$  have been squeezed and confirmed by elemental analyses and TGA (Figure S8), which is in agreement with squeeze electrons in P1 Unit Cell : 526, equal to  $16[\text{HN}(\text{CH}_3)_2]$  and  $16[\text{H}_2\text{O}]$ .

## 1.2 Catalytic activity tests

The hydrogenation reduction of nitroarenes to anilines with hydrazine hydrate in the presence of  $\gamma$ -1 was investigated as a benchmark system for the optimization of the conditions. The effects of the solvent, cycle number, reaction time and temperature were evaluated (see also the Supporting Information).

General procedure for the reduction of nitrobenzene: Nitrobenzene (10  $\mu\text{L}$ , 0.097 mmol), EtOH (2 mL) and  $\gamma$ -1 (7.5 mg, 3 mol %, 0.0029 mmol) were added into a 25 mL round bottomed flask with magnetic stirring. Then,  $\text{N}_2\text{H}_4 \cdot \text{H}_2\text{O}$  (85%) (20  $\mu\text{L}$ , 0.3 mmol) were added into the reactor and heated to reflux with stirring at  $80^\circ\text{C}$  for 2 hours. The reaction was complete (incomplete or messy) detected by TLC (n-hexane/ethyl acetate = 5:1). The samples were obtained by centrifugation and filtration and analyzed by Shimadzu GC 2014C. The filtrate has been diluted to 4mL with EtOH and analyzed by ICP to determine the molybdenum amount to confirm the heterogeneous catalysis reaction. Recycled catalyst analyzed by IR spectrum after centrifugal separation was used in the same manner as with fresh catalyst to determine the reusability of the catalyst as a hydrogenation agent (Figure S11, S12). Recycle experiment also conducted under similar conditions except for appropriate adjustment in the amount of hydrazine hydrate used and the reaction time for completely conversion (Figure 2 left). The amount of hydrazine hydrate added and the reaction time needed in each cycle is 20  $\mu\text{L}$ , 2 hours (fresh catalyst); 20  $\mu\text{L}$ , 3 hours (cycle 1); 40  $\mu\text{L}$ , 4 hours (cycle 2); 40  $\mu\text{L}$ , 5 hours (cycle 3); 60  $\mu\text{L}$  6 hours (cycle 4) and 100  $\mu\text{L}$  10 hours (cycle 5) respectively.

The reduction of nitrobenzene to aniline in this catalytic systems based on different molybdenum cluster compounds (3a, 3b, 4a, 4b) has been conducted for performance comparisons and mechanism study (Figure 2 right). Reaction conditions: catalyst (3 mol %),  $\text{PhNO}_2$  (10  $\mu\text{L}$ , 0.097 mmol),  $\text{N}_2\text{H}_4 \cdot \text{H}_2\text{O}$  (20  $\mu\text{L}$ , 0.3 mmol), solvent (2 mL),  $80^\circ\text{C}$ , 2 h. no: only EtOH. 3a:  $[\text{Mo}^{\text{IV}}_3\text{O}_2(\text{O}_2\text{CCH}_3)_6(\text{H}_2\text{O})_3]\text{ZnCl}_4$ ; 3b:  $[\text{Mo}^{\text{IV}}_3\text{O}_2(\text{O}_2\text{CCH}_3)_6\text{py}_3]\text{ZnCl}_4$ ; 4a:  $[\text{Pro}_4\text{N}]_2[\text{Mo}^{\text{IV}}_3\text{O}_4(\text{C}_2\text{O}_4)_3(\text{H}_2\text{O})_3]$ ; 4b:  $[\text{Pro}_4\text{N}]_2[\text{Mo}^{\text{IV}}_3\text{O}_4(\text{C}_2\text{O}_4)_3\text{py}_3]$ .

To determine the yield of isolated products for different functionalized anilines, the general procedure was scaled up by the factor of three. After full conversion was achieved, the resultant suspension was centrifugated and filtered through filter paper and the solvent of the filtrate was removed by rotary evaporator and dissolved in deuterated solvents ( $\text{CDCl}_3$ ) for NMR analysis. In a general protocol, reaction time usually extends to 3-4 hours, detected by TLC (n-hexane/ethyl acetate = 5:1  $\rightarrow$  2:1) to ensure reaction complete conversion.

## 2. DFT theoretical calculations

DFT calculations were performed using the GAUSSIAN 09 program package (Revision D.01)<sup>30</sup> and crystal structure parameters. DFT calculations were carried out using the (U)B3LYP functional, that is, Beck's hybrid three-parameter exchange functional<sup>31</sup> with the Lee-Yang-Parr correlation functional.<sup>32</sup> In these calculations, the solvent effects were taken into account by the Polarizable Continuum Model (PCM).<sup>33</sup> The natural atomic orbital(NAO) analyses were calculated by the NBO 3.1 module embedded in Gaussian 09 program.

The analyses of frontier molecular orbitals and spin densities were performed by Multiwfn<sup>34</sup>, which is a multifunctional wavefunction analysis program developed by Lu et. al. and can be freely downloaded.

## 3. Figures

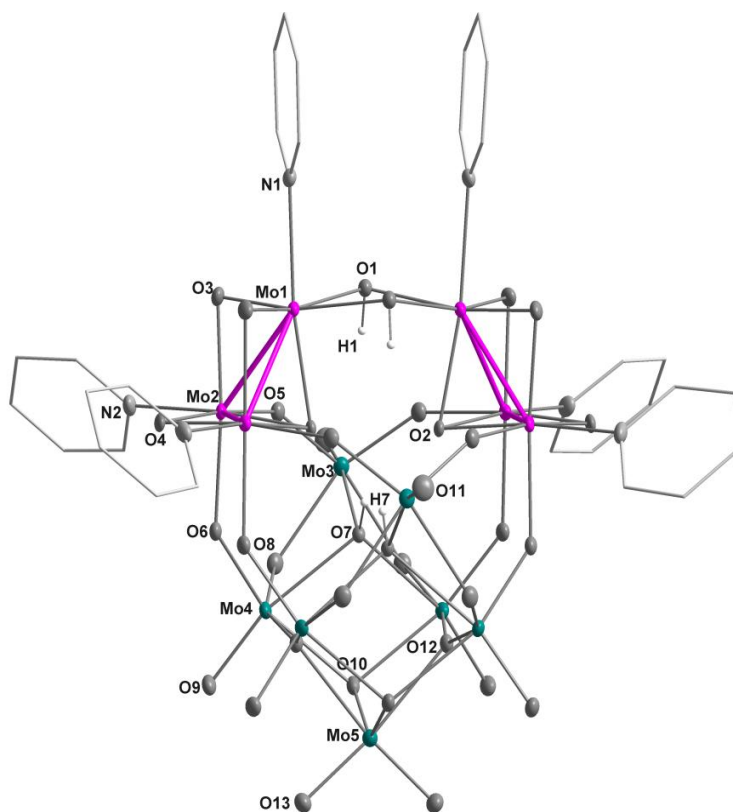


**Figure S1.** Structure of  $\gamma$ -[H<sub>4</sub>Mo<sup>IV</sup><sub>6</sub>Mo<sup>VI</sup><sub>7</sub>O<sub>36</sub>py<sub>6</sub>]<sup>2-</sup> ( $\gamma$ -**1a**) (Mo<sup>IV</sup>, purple; Mo<sup>VI</sup>, blue) with 30% probability thermal ellipsoids for non-carbon atoms.

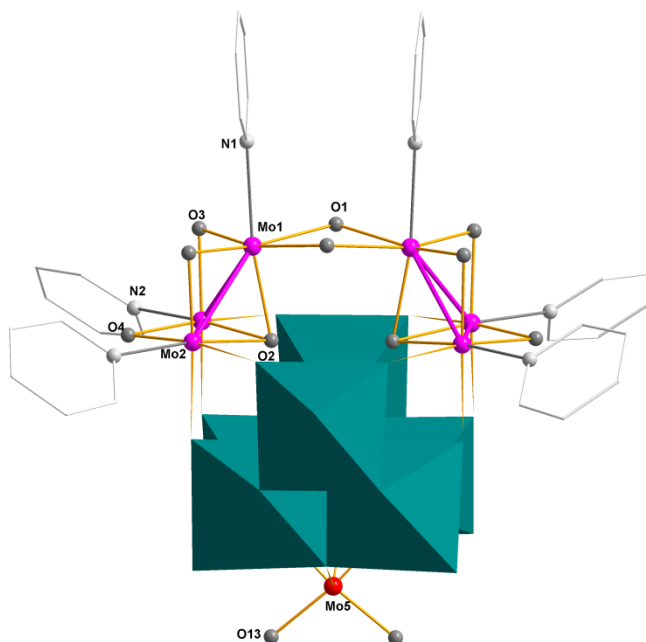
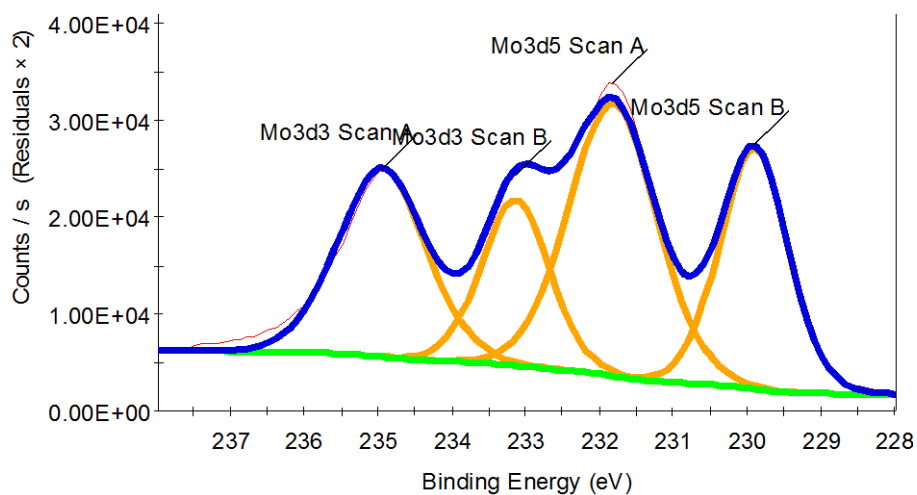


**Figure S2.** Partly polyhedral (Mo<sup>VI</sup>) presentation of  $\gamma$ -**1a** showing a model of the low-valence Mo(IV) clusters supported on a Mo(VI) oxide of the highest oxidation state.



Binding energies of Mo 3d from the literatures<sup>35-38</sup> and the binding energies of peaks used to assign species from the present measurements of  $\gamma$ -1.

| Oxidation state                                    | Mo 3d <sub>5/2</sub> | Mo 3d <sub>3/2</sub> |
|----------------------------------------------------|----------------------|----------------------|
| Mo <sup>VI</sup> -Na <sub>2</sub> MoO <sub>4</sub> | 231.9                | 235.4                |
| Mo <sup>IV</sup> O(OH) <sub>2</sub>                | 230. 2               | 233.4                |
| Mo <sup>IV</sup> - $\beta$ -2                      | 230.0                | 233.2                |
| Mo <sup>VI</sup> - $\beta$ -2                      | 231.9                | 235.05               |
| Mo <sup>IV</sup> - $\gamma$ -1 (B)                 | 229.90               | 233.13               |
| Mo <sup>VI</sup> - $\gamma$ -1 (A)                 | 231.81               | 234.94               |

**Figure S3.** XPS of  $\gamma$ -1.

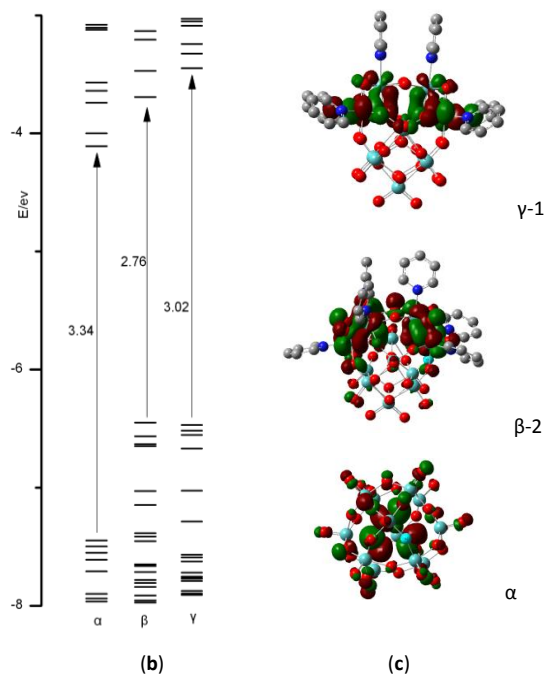
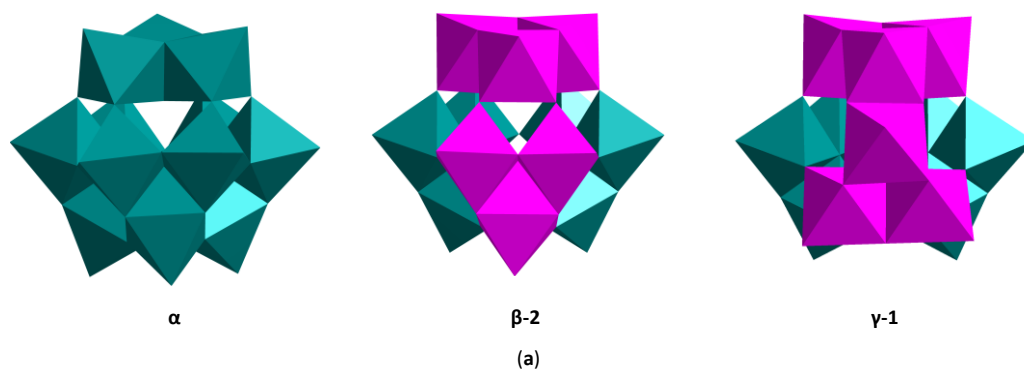


**Figure S4.** (a)  $\alpha \rightarrow \beta \rightarrow \gamma$  Keggin structure evolution induced by  $60^\circ$  rotation of top  $\text{Mo}^{\text{IV}}_3\text{O}_{13}$  set (marked in pink polyhedron) followed by belt  $\text{Mo}^{\text{IV}}_3\text{O}_{13}$  set. (b) comparison of HOMO energy levels and HOMO-LUMO gap of  $\alpha$ - $[\text{H}_4\text{Mo}^{\text{VI}}_{12}\text{O}_{40}]^{4-}$ , 12e-reduced  $\beta$ -2 and  $\gamma$ -1 Keggin anions. (c) HOMO orbitals of  $\alpha$ -,  $\beta$ -2 and  $\gamma$ -1 Keggin anions.

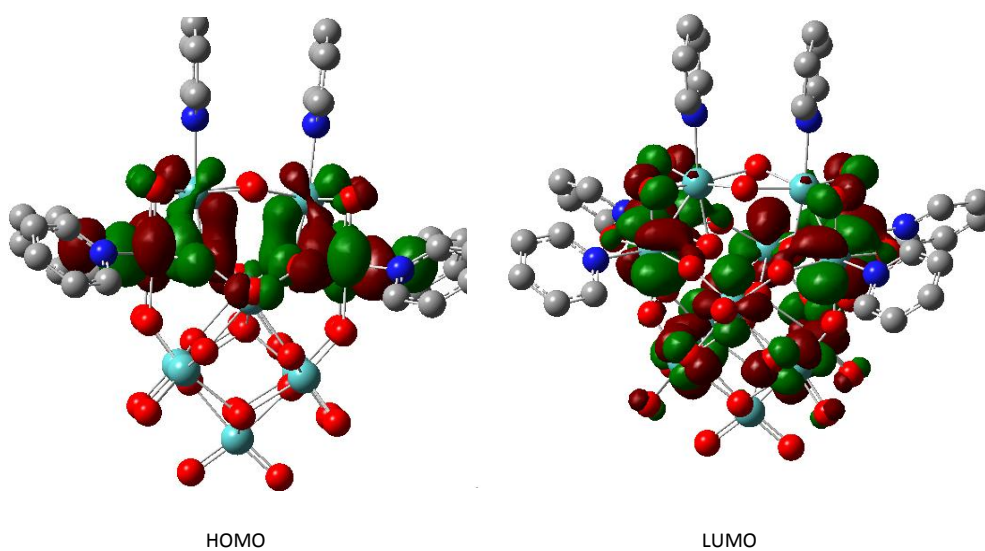


**Figure S5.** HOMO and LUMO of  $\gamma$ -1.

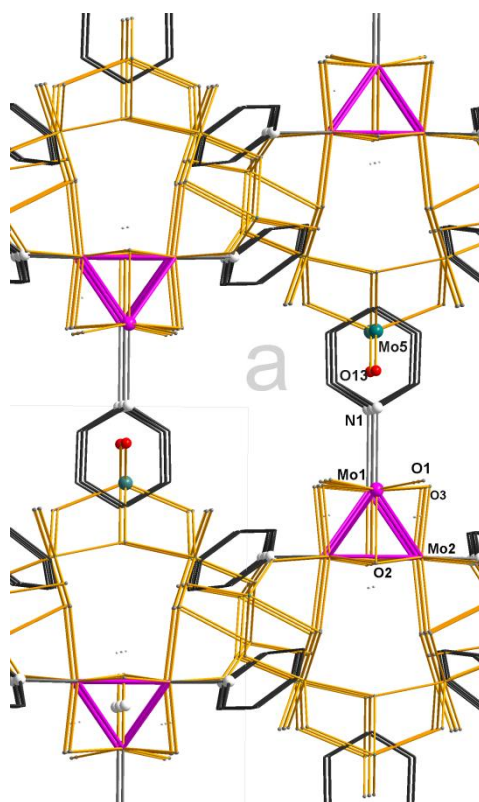


**Figure S6.** Crystal structure of  $\gamma$ -1 along  $a$  axis showing that the  $\text{Mo}^{\text{VI}}\text{O}_2$  groups (Mo5, O13) are on the top of the  $\text{Mo}^{\text{IV}}(\mu_2\text{-OH})_2$  active site (Mo1, O1).

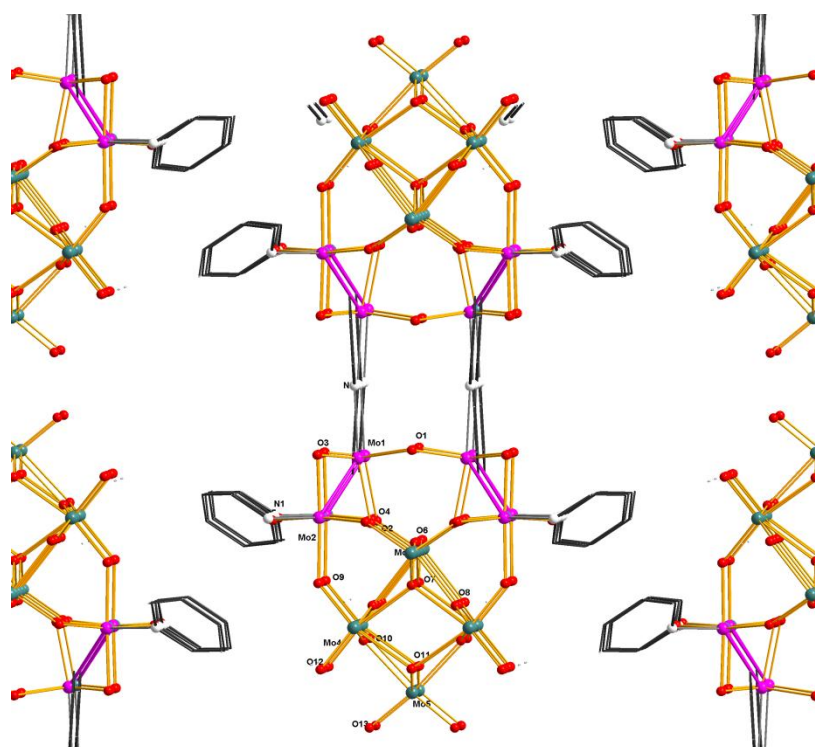


**Figure S7.** Crystal structure of  $\gamma$ -1 along  $c$  axis showing that the  $\text{Mo}^{\text{VI}}\text{O}_2$  groups (Mo5, O13) are close to the  $\text{Mo}^{\text{IV}}(\mu_2\text{-OH})_2$  active site (Mo1, O1).

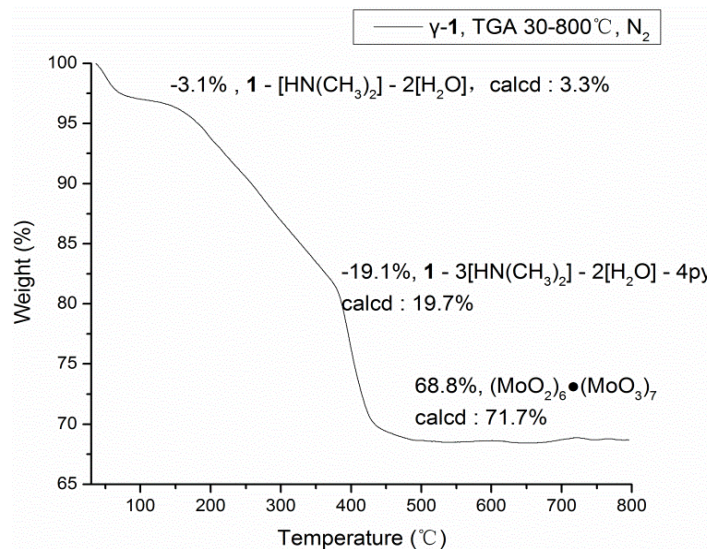


Figure S8. TGA of  $\gamma$ -1.

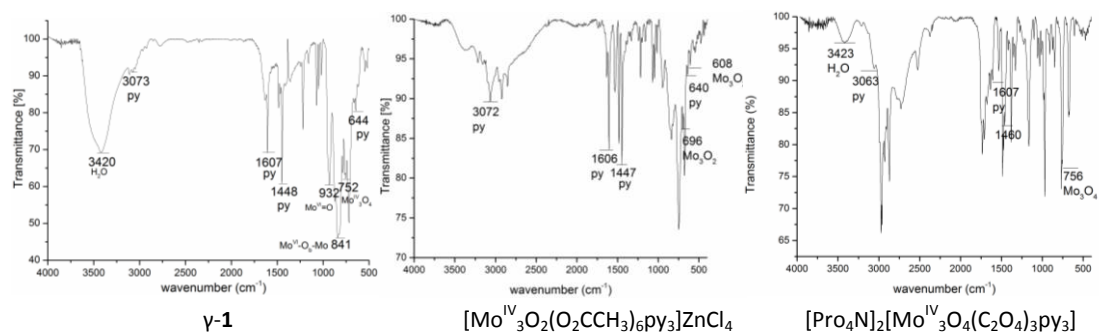


Figure S9. IR of  $\gamma$ -1,  $[\text{Mo}^{\text{IV}}_3\text{O}_2(\text{O}_2\text{CCH}_3)_6\text{py}_3]\text{ZnCl}_4$  and  $[\text{Pro}_4\text{N}]_2[\text{Mo}^{\text{IV}}_3\text{O}_4(\text{C}_2\text{O}_4)_3\text{py}_3]$ .

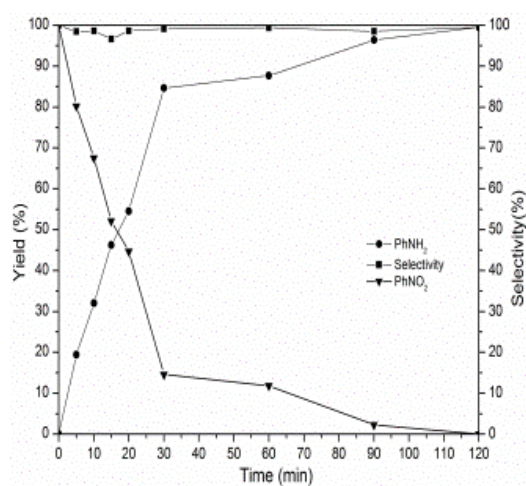
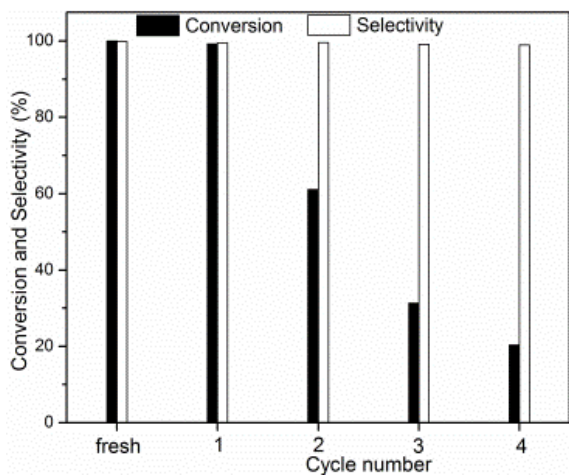
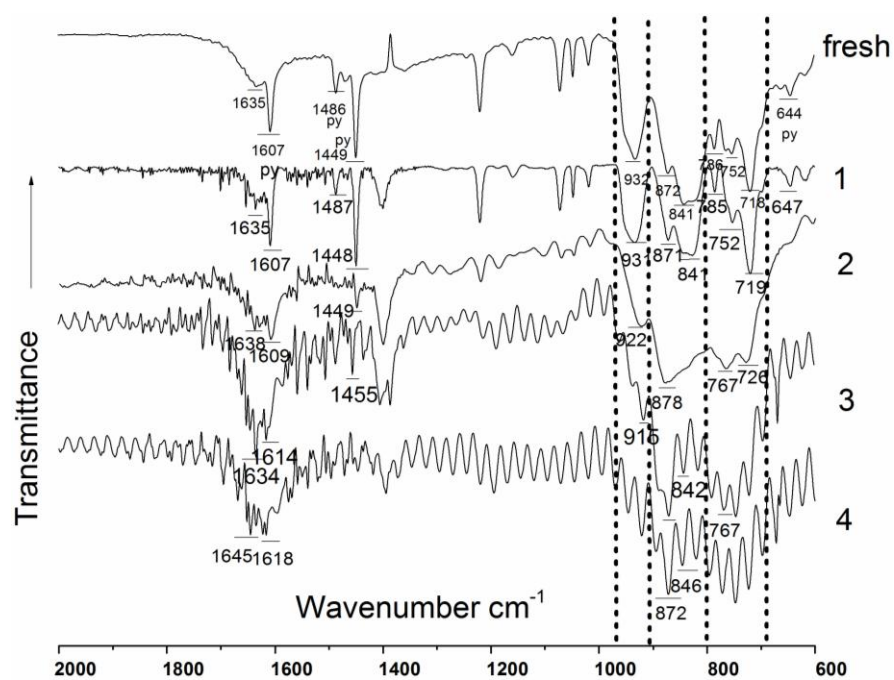


Figure S10. Time-dependent profiles for the reduction of nitrobenzene to aniline.

Reaction conditions:  $\gamma$ -1 (7.5 mg, 3 mol %),  $\text{PhNO}_2$  (10  $\mu\text{L}$ , 0.097 mmol),  $\text{N}_2\text{H}_4 \cdot \text{H}_2\text{O}$  (20  $\mu\text{L}$ , 0.3 mmol), EtOH (2 mL),  $80^{\circ}\text{C}$ .



**Figure S11.** Cycle number profiles for the reduction of nitrobenzene to aniline catalyzed by reused  $\gamma$ -1. Reaction conditions: recycled catalyst (7.5 mg, 3 mol %),  $\text{PhNO}_2$  (10  $\mu\text{L}$ , 0.097 mmol),  $\text{N}_2\text{H}_4 \cdot \text{H}_2\text{O}$  (20  $\mu\text{L}$ , 0.3 mmol), EtOH (2 mL), 80°C.



**Figure S12.** FTIR for fresh and used catalysts: (fresh)  $\gamma$ -1, (1) after the first used, (2) after the second used, (3) after the third used, (4) after the fourth used.

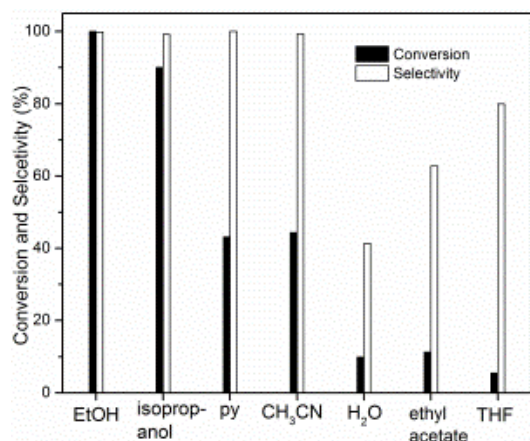
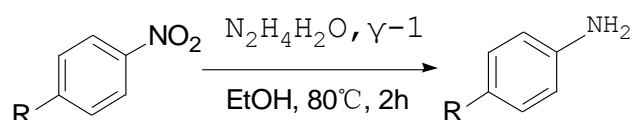


**Figure S13.** Solvent-dependent performance profiles of  $\gamma$ -1 for the reduction of nitrobenzene to aniline. Reaction conditions:  $\gamma$ -1 (7.5 mg, 3 mol %),  $\text{PhNO}_2$  (10  $\mu\text{L}$ , 0.097 mmol),  $\text{N}_2\text{H}_4\cdot\text{H}_2\text{O}$  (20  $\mu\text{L}$ , 0.3 mmol), solvent (2 mL), 80  $^\circ\text{C}$ , 2 h.

#### 4. Tables

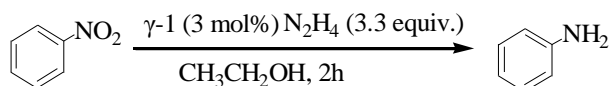


| entry | R                  | Conversion(%) <sup>j</sup> | Yield(%) <sup>j</sup> |
|-------|--------------------|----------------------------|-----------------------|
| 1     | H                  | 100                        | >99.8                 |
| 2     | Br                 | 100                        | >99.8                 |
| 3     | CH <sub>3</sub>    | 100                        | >99.8                 |
| 4     | COOCH <sub>3</sub> | 100                        | >99.8                 |
| 5     | H <sup>a</sup>     | 99.2                       | 98.7                  |
| 6     | H <sup>b</sup>     | 61.1                       | 61.1                  |
| 7     | H <sup>c</sup>     | 31.3                       | 31.1                  |
| 8     | H <sup>d</sup>     | 20.4                       | 20.2                  |
| 9     | H <sup>e</sup>     | 100                        | 100                   |
| 10    | H <sup>f</sup>     | 100                        | 100                   |
| 11    | H <sup>g</sup>     | 99.4                       | 99.4                  |
| 12    | H <sup>h</sup>     | 98.1                       | 98                    |
| 13    | H <sup>i</sup>     | 100                        | 100                   |

**Table S1.** Hydrogenation Reduction of Nitrobenzene to Aniline with the Hybridized Keggin Cluster  $\gamma$ -1.

Reaction conditions:  $\gamma$ -1 (7.5 mg, 3%),  $\text{ArNO}_2$  (0.097 mmol),  $\text{N}_2\text{H}_4\cdot\text{H}_2\text{O}$  (85%, 20  $\mu\text{L}$ ), EtOH (2 mL), 80  $^\circ\text{C}$ , 2 h.

<sup>a</sup> one cycle; <sup>b</sup> two cycle; <sup>c</sup> three cycle; <sup>d</sup> four cycle; <sup>e</sup> one cycle with  $\text{N}_2\text{H}_4\cdot\text{H}_2\text{O}$  (85%, 20  $\mu\text{L}$ ), 3 h; <sup>f</sup> two cycle with  $\text{N}_2\text{H}_4\cdot\text{H}_2\text{O}$  (85%, 40  $\mu\text{L}$ ), 4 h; <sup>g</sup> three cycle with  $\text{N}_2\text{H}_4\cdot\text{H}_2\text{O}$  (85%, 40  $\mu\text{L}$ ), 5 h; <sup>h</sup> four cycle with  $\text{N}_2\text{H}_4\cdot\text{H}_2\text{O}$  (85%, 60  $\mu\text{L}$ ), 6 h; <sup>i</sup> five cycle with  $\text{N}_2\text{H}_4\cdot\text{H}_2\text{O}$  (85%, 100  $\mu\text{L}$ ), 10 h; <sup>j</sup> GC yield.



| entry            | Temperature(°C) | Conversion(%) <sup>[b]</sup> | Yield(%) <sup>[b]</sup> |
|------------------|-----------------|------------------------------|-------------------------|
| 1                | R.T.            | 5.8                          | 5.8                     |
| 2                | 70              | 70.4                         | 70.4                    |
| 3                | 80              | >99                          | >99                     |
| 4 <sup>[c]</sup> | 80              | -                            | -                       |

**Table S2.** Influence of the temperature on the catalytic reduction of nitrobenzene to aniline.<sup>[a]</sup>

[a] Reaction conditions: Nitrobenzene (10  $\mu$ L, 0.097 mmol),  $N_2H_4 \cdot H_2O$  (20 $\mu$ L, 0.3mmol), 3 mol% catalyst (7.5 mg), EtOH (2 mL), 2 h. [b] Determined by GC. [c] Without catalyst.

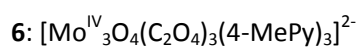
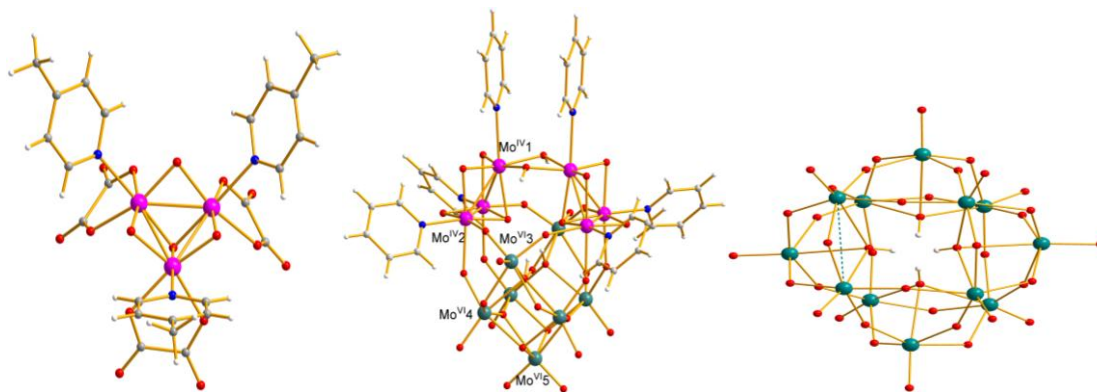
**Table S3.** Bond valance sum analyses for  $\gamma$ -1

| Atom | Coord | D_aver      | Sigm | Distort(x10-4) | Valence | BVSum(Sigma) |
|------|-------|-------------|------|----------------|---------|--------------|
| Mo1  | 6.00  | 2.0565( 11) |      | 71.440         | 4.000   | 4.325( 12)   |
| Mo2  | 6.00  | 2.0452( 10) |      | 29.465         | 4.000   | 4.352( 13)   |
| Mo3  | 6.00  | 1.9608( 12) |      | 104.293        | 6.000   | 5.970( 23)   |
| Mo4  | 6.00  | 1.9558( 9)  |      | 73.123         | 6.000   | 5.789( 16)   |
| Mo5  | 6.00  | 1.9752( 13) |      | 111.332        | 6.000   | 5.858( 25)   |
| O1   | 2.00  | 2.0332( 13) |      | 0.000          | -2.000  | 1.343( 5)    |
| O2   | 3.00  | 2.0166( 14) |      | 29.019         | -2.000  | 2.193( 8)    |
| O3   | 2.00  | 1.9689( 17) |      | 26.310         | -2.000  | 1.658( 8)    |
| O4   | 2.00  | 1.8658( 16) |      | 0.000          | -2.000  | 2.112( 9)    |
| O5   | 2.00  | 1.9299( 17) |      | 50.268         | -2.000  | 1.974( 9)    |
| O6   | 2.00  | 2.0103( 16) |      | 78.120         | -2.000  | 1.665( 8)    |
| O7   | 3.00  | 2.2080( 14) |      | 0.073          | -2.000  | 1.330( 5)    |
| O8   | 2.00  | 1.9908( 17) |      | 46.767         | -2.000  | 1.704( 8)    |
| O9   | 1.00  | 1.7342( 25) |      | 0.000          | -2.000  | 1.595( 11)   |
| O10  | 3.00  | 2.0940( 14) |      | 6.888          | -2.000  | 1.830( 7)    |
| O11  | 1.00  | 1.7082( 41) |      | 0.000          | -2.000  | 1.711( 19)   |
| O12  | 3.00  | 2.0537( 11) |      | 27.996         | -2.000  | 2.100( 5)    |
| O13  | 1.00  | 1.7019( 35) |      | 0.000          | -2.000  | 1.741( 16)   |
| N1   | 1.00  | 2.3665( 42) |      | 0.000          | -3.000  | 0.417( 5)    |
| N2   | 1.00  | 2.1410( 37) |      | 0.000          | -3.000  | 0.767( 8)    |

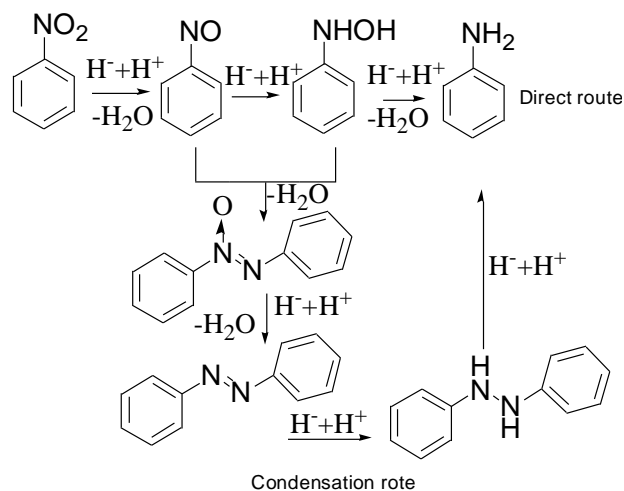
**Table S4.** DFT-calculated Mulliken charges of  $Mo^{VI}$  in **5**,  $Mo^{IV}/Mo^{VI}$  in  $\gamma$ -1 and  $Mo^{IV}$  in **6**<sup>39</sup>, which reveal remarkable electron transfer among  $Mo^{IV}$  and  $Mo^{VI}$  in  $\gamma$ -1.

|         | <b>6</b>  | $\gamma$ -1 |            |            |            |            | <b>5</b>  |
|---------|-----------|-------------|------------|------------|------------|------------|-----------|
| Mo atom | $Mo^{IV}$ | $Mo^{IV1}$  | $Mo^{IV2}$ | $Mo^{VI3}$ | $Mo^{VI4}$ | $Mo^{VI5}$ | $Mo^{VI}$ |

|                   |       |        |        |        |       |        |       |
|-------------------|-------|--------|--------|--------|-------|--------|-------|
| Mulliken charge   | 0.931 | 1.095  | 1.056  | 1.386  | 1.558 | 1.306  | 1.552 |
| electron transfer |       | +0.164 | +0.125 | -0.166 | -     | -0.246 |       |



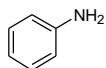
## 5. Scheme



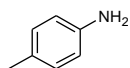
**Scheme S1.** Reaction network of the nitrobenzene reduction.<sup>40</sup>

The condensation route involves the azobenzene intermediate. When azobenzene (0.0485 mmol, 8.9 mg) was used as reactant,  $\gamma$ -1 (3 mol %, 7.5 mg) offered 11.6% conversion at 80 °C in 2 h (the reaction conditions similar to  $\text{PhNO}_2$  with 0.097 mmol). The conversion of  $\text{PhNO}_2$  over  $\gamma$ -1 was 7.6 times greater than the azobenzene conversion that we believe the reaction occurred mainly via the direct route with multi-step process.

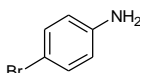
## 6. Characterization data of the isolated products.



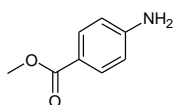
**Aniline:** isolated yield: 95%.  $^1\text{H}$  NMR (400 MHz,  $\text{CDCl}_3$ )  $\delta$  7.17 (t,  $J = 7.8$  Hz, 2H), 6.83 – 6.63 (m, 3H), 3.49 (s, 2H);  $^{13}\text{C}$  NMR (101 MHz,  $\text{CDCl}_3$ )  $\delta$  146.33, 129.26, 118.54, 115.08.



**4-methylaniline:** isolated yield: 96%.  $^1\text{H}$  NMR (400 MHz,  $\text{CDCl}_3$ )  $\delta$  6.98 (d,  $J = 8.2$  Hz, 2H), 6.62 (d,  $J = 8.2$  Hz, 2H), 3.30 (s, 2H), 2.26 (s, 3H);  $^{13}\text{C}$  NMR (101 MHz,  $\text{CDCl}_3$ )  $\delta$  143.76, 129.71, 127.67, 115.23, 20.40.

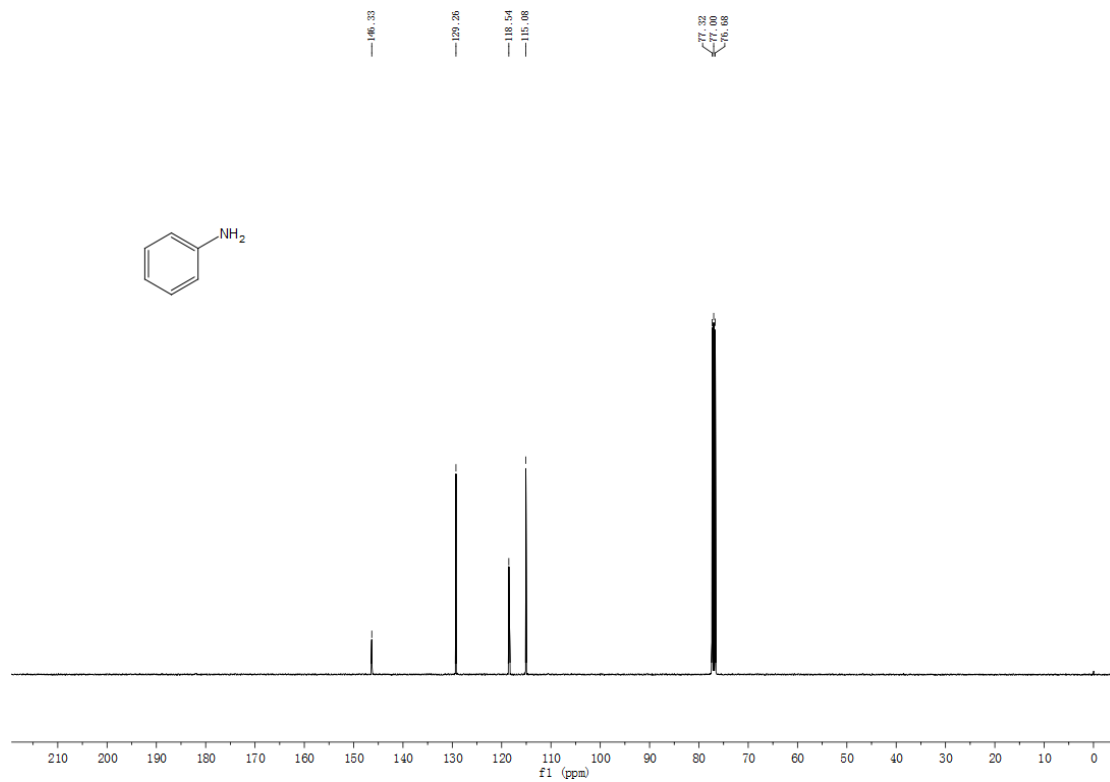
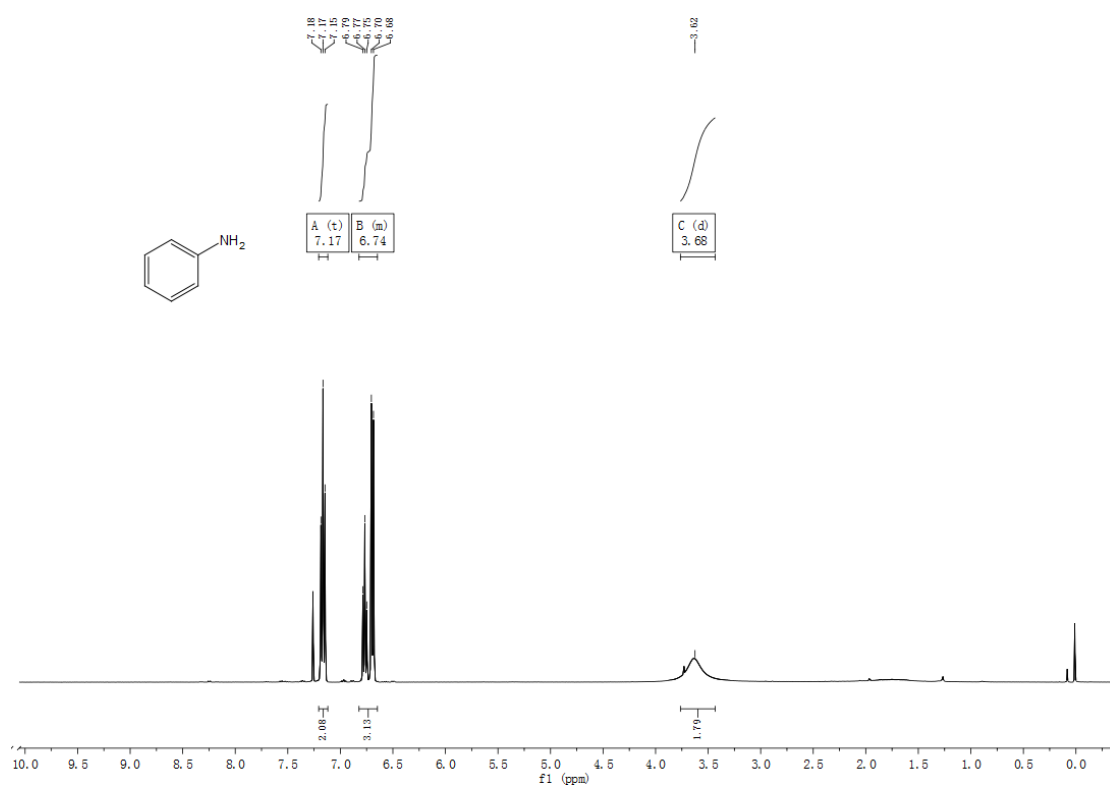


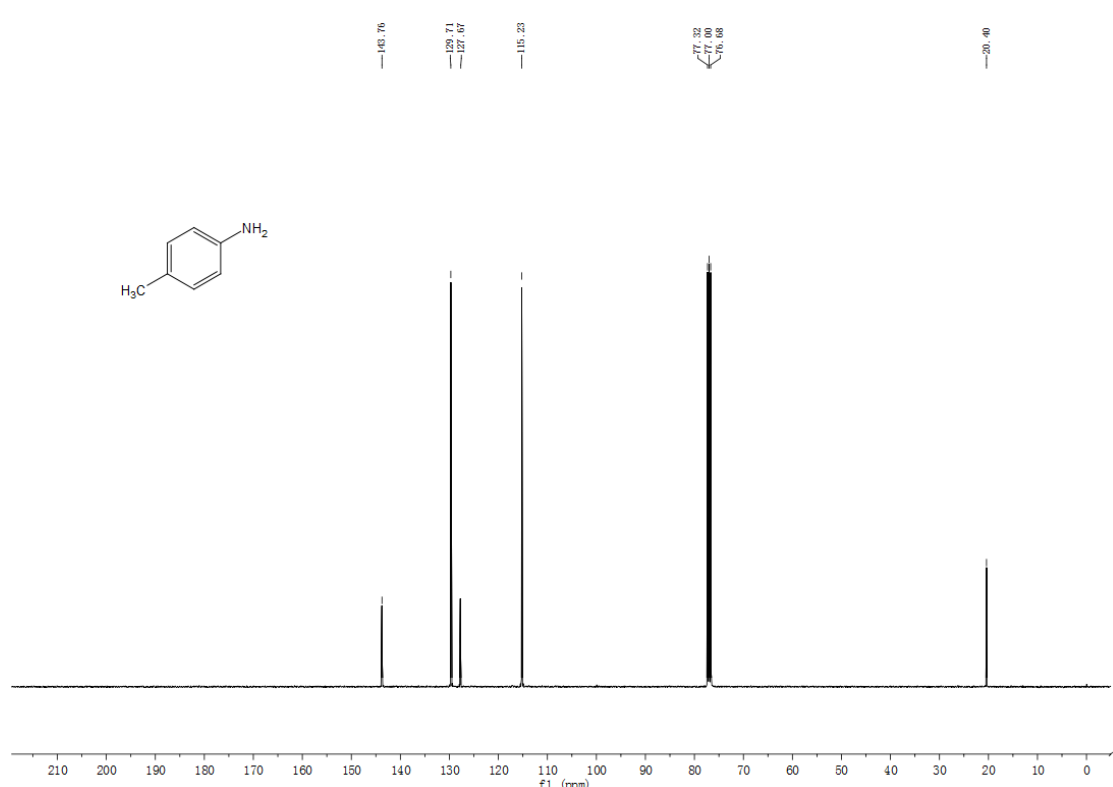
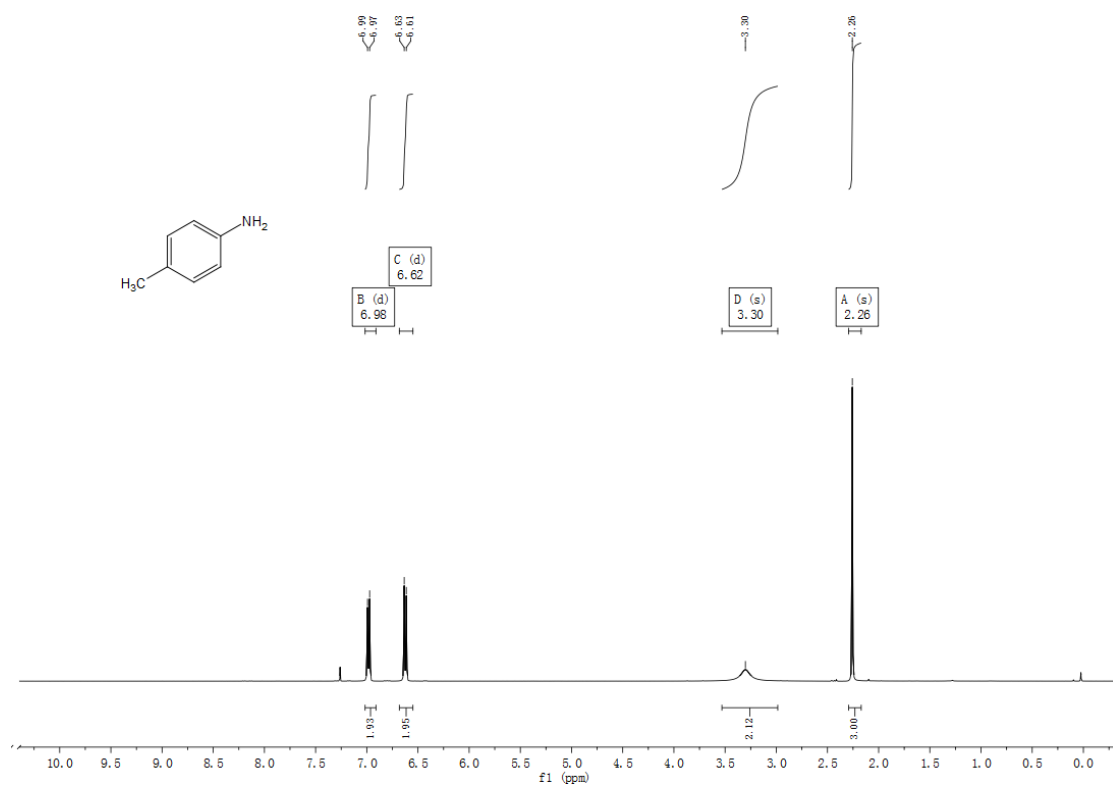
**4-bromoaniline:** isolated yield: 98%.  $^1\text{H}$  NMR (400 MHz,  $\text{CDCl}_3$ )  $\delta$  7.26 – 7.20 (m, 2H), 6.60 – 6.50 (m, 2H), 3.50 (s, 2H);  $^{13}\text{C}$  NMR (101 MHz,  $\text{CDCl}_3$ )  $\delta$  145.35, 131.94, 116.67, 110.13.

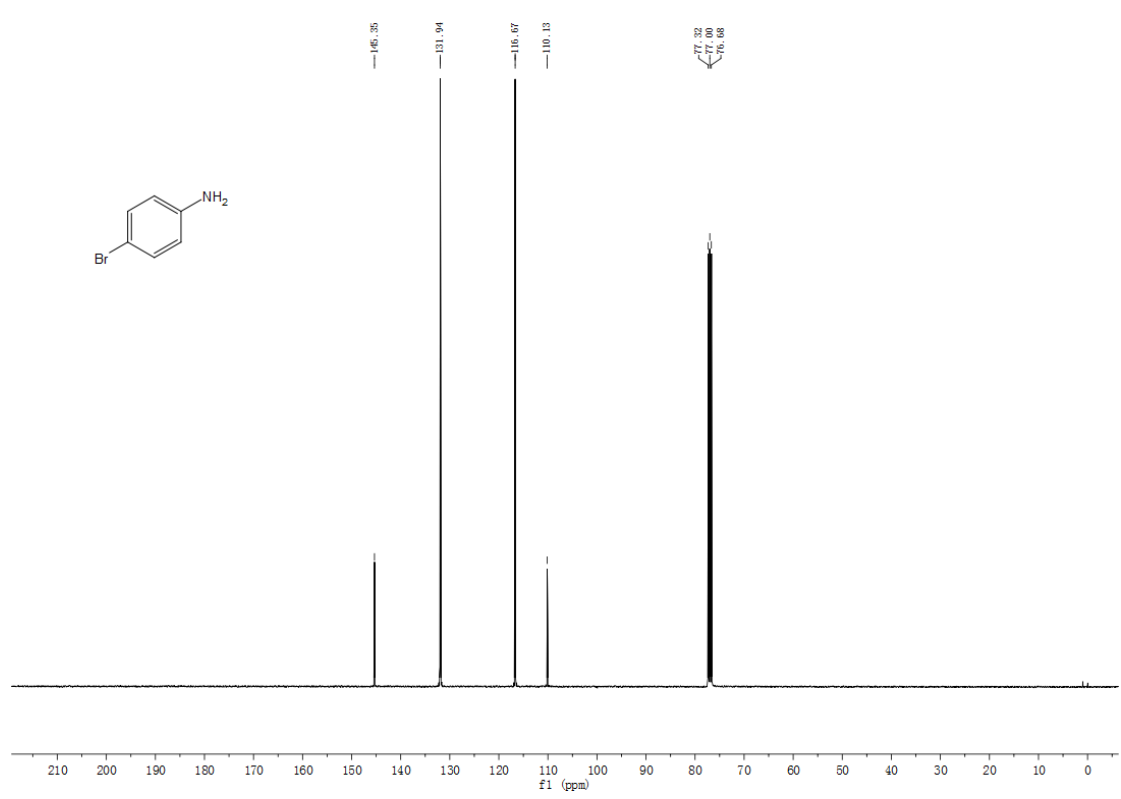
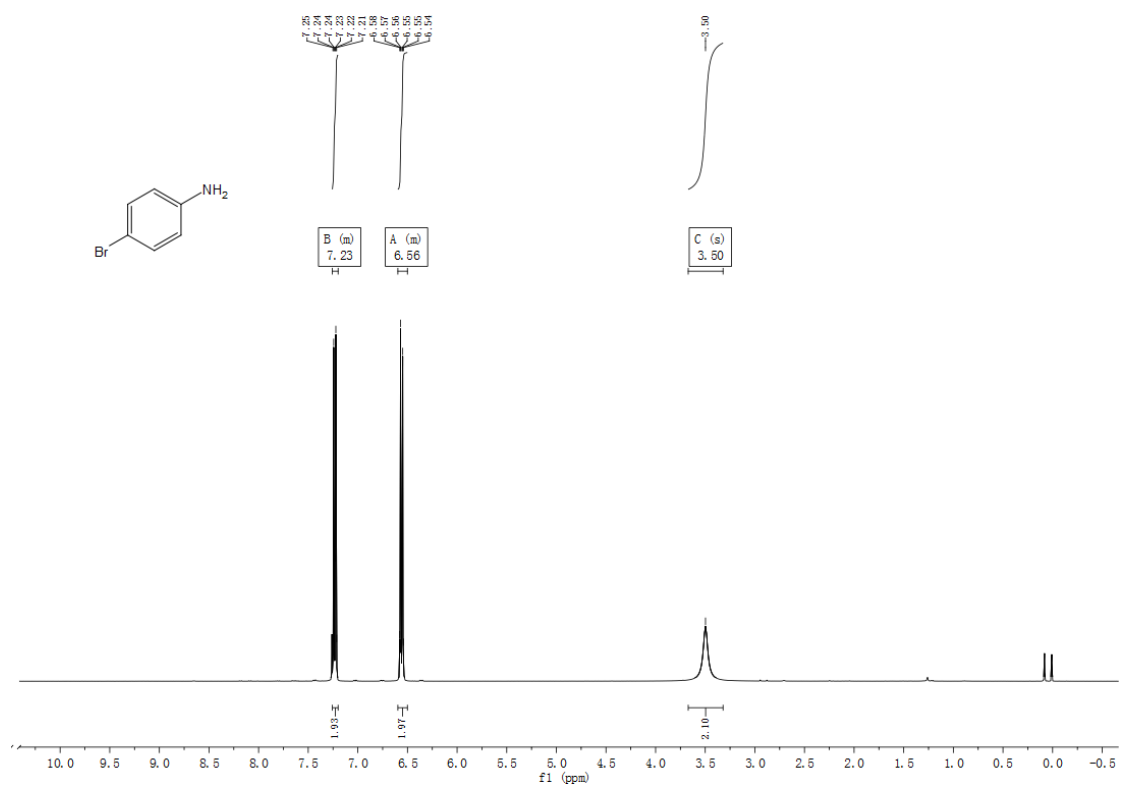


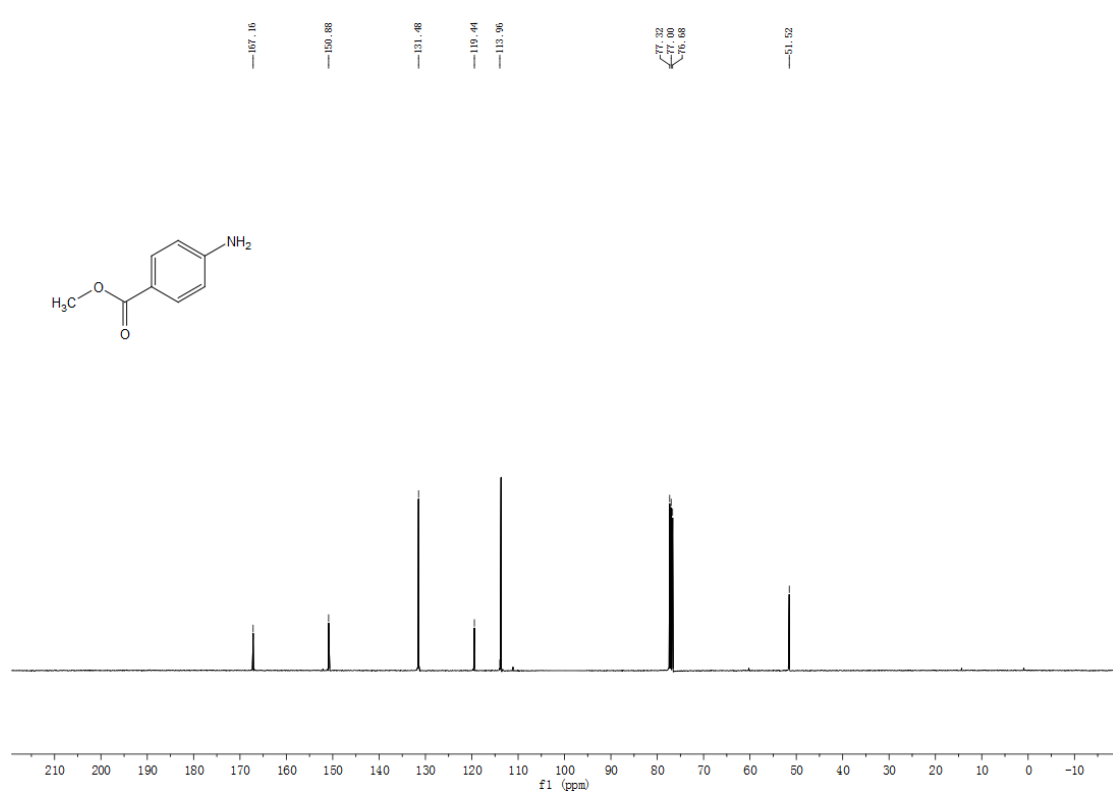
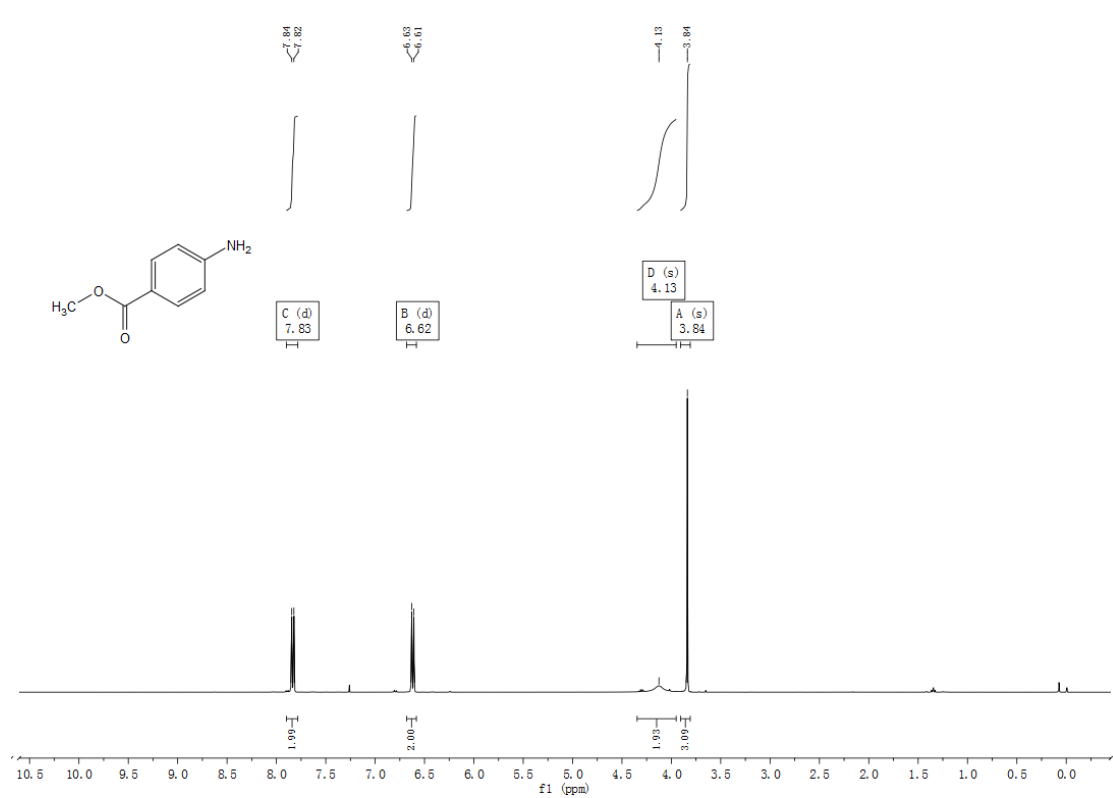
**methyl 4-aminobenzoate:** isolated yield: 96%.  $^1\text{H}$  NMR (400 MHz,  $\text{CDCl}_3$ )  $\delta$  7.83 (d,  $J = 8.7$  Hz, 2H), 6.62 (d,  $J = 8.7$  Hz, 2H), 4.13 (s, 2H), 3.84 (s, 3H);  $^{13}\text{C}$  NMR (101 MHz,  $\text{CDCl}_3$ )  $\delta$  167.16 (s), 150.88 (s), 131.48 (s), 119.44 (s), 113.96 (s), 51.52 (s).

### 7. <sup>1</sup>H NMR and <sup>13</sup>C NMR spectra of the isolated products.









## 8. References.

- [27] Sheldrick, G.M. (2015) "Crystal structure refinement with SHELXL", *Acta Cryst.*, 2015, **C71**, 3-8.
- [28] A. Birnbaum, F. A. Cotton, Z. Dori, D. O. Marler, G. M. Reisner, W. Schwotzer and M. Shaia, *Inorg. Chem.*, 1983, **22**, 2723-2726.
- [29] J. Zhao and L. Xu, *Inorg. Chem. Commun.*, 2008, **11**, 353-357.
- [30] Gaussian 09, Revision D.01, Frisch, M. J.; Trucks, G. W.; Schlegel, H. B.; Scuseria, G. E.; Robb, M. A.; Cheeseman, J. R.; Scalmani, G.; Barone, V.; Mennucci, B.; Petersson, G. A.; Nakatsuji, H.; Caricato, M.; Li, X.; Hratchian, H.P.; Izmaylov, A. F.; Bloino, J.; Zheng, G.; Sonnenberg, J. L.; Hada, M.; Ehara, M.; Toyota, K.; Fukuda, R.; Hasegawa, J.; Ishida, M.; Nakajima, T.; Honda, Y.; Kitao, O.; Nakai, H.; Vreven, T.; Montgomery, J. A.; Peralta, J. E.; Ogliaro, F.; Bearpark, M.; Heyd, J. J.; Brothers, E.; Kudin, K. N.; Staroverov, V. N.; Kobayashi, R.; Normand, J.; Raghavachari, K.; Rendell, A.; Burant, J. C.; Iyengar, S. S.; Tomasi, J.; Cossi, M.; Rega, N.; Millam, J. M.; Klene, M.; Knox, J. E.; Cross, J. B.; Bakken, V.; Adamo, C.; Jaramillo, J.; Gomperts, R.; Stratmann, R. E.; Yazyev, O.; Austin, A. J.; Cammi, R.; Pomelli, C.; Ochterski, J. W.; Martin, R. L.; Morokuma, K.; Zakrzewski, V. G.; Voth, G. A.; Salvador, P.; Dannenberg, J. J.; Dapprich, S.; Daniels, A. D.; Farkas, Ö.; Foresman, J. B.; Ortiz, J. V.; Cioslowski, J.; Fox, D. J.; *Gaussian, Inc., Wallingford CT*, 2009.
- [31] A. D. Becke, *J. Chem. Phys.* 1993, **98**, 5648-5652.
- [32] C. Lee, W. T. Yang and R. G. Parr, *Phys. Rev. B.* 1988, **37**, 785-789.
- [33] (a) M. Cossi, G. Scalmani, N. Rega and V. Barone, *J. Chem. Phys.* 2002, **117**, 43-54; (b) V. Barone, M. Cossi and J. Tomasi, *J. Chem. Phys.* 1997, **107**, 3210-3221.
- [34] (a) T. Lu and F. W. Chen, *J. Mol. Graph. Model.* 2012, **38**, 314-323; (b) Multiwfn software can be freely downloaded from website: <http://multiwfn.codeplex.com/>.
- [35] B. Brox and I. Olefjord, *Surf. Interface Anal.* 1988, **13**, 3-6.
- [36] C. R. Clayton and Y. C. Lu, *Surf. Interface Anal.* 1989, **14**, 66-70.
- [37] Y. C. Lu and C.R. Clayton, *Corros. Sci.* 1989, **29**, 927-937.
- [38] I. A. Okonkwo, J. Doff, A. Baron-Wiecheć, G. Jones, E. V. Koroleva, P. Skeldon and G. E. Thompson, *Thin Solid Films*, 2012, **520**, 6318-6327.
- [39] B. Modéc and P. Bukovec, *Inorg. Chim. Acta.*, 2015, **424**, 226-234.
- [40] (a) F. Haber, *Z. Elektrochem, Angew. Phys. Chem.*, 1898, **22**, 506-514; (b) C. F. Zhang, Z. X. Zhang, X. Wang, M. R. Li, J. M. Lu, R. Si, F. Wang, *Appl. Catal. A: Gen.*, 2016, **525**, 85-93; (c) C. F. Zhang, X. Wang, M. R. Li, Z. X. Zhang, Y. H. Wang, R. Si, F. Wang, *Chin. J. Catal.*, 2016, **37**, 1569-1577.